Available online at www.sciencedirect.com
ScienceDirect
International Journal of Thermal Sciences 46 (2007) 936–943
International Journal of Thermal Sciences
www.elsevier.com/locate/ijts

A numerical investigation on NO_X formation in counterflow *n*-heptane triple flames

Hongsheng Guo *, Gregory J. Smallwood

Institute for Chemical Process and Environmental Technology, National Research Council of Canada, 1200 Montreal Road, Ottawa, Ontario, Canada K1A 0R6

Received 9 February 2006; received in revised form 1 November 2006; accepted 5 November 2006

Available online 4 December 2006

Abstract

The formation of NO_X in counterflow *n*-heptane/air triple flames was investigated by numerical simulation. Detailed chemistry and complex thermal and transport properties were employed. The results indicate that a triple flame produces more NO and NO_2 than the corresponding premixed flames due to not only the appearance of the diffusion flame but also the interaction between different flame branches. The relative contributions of different routes to NO formation in the premixed flame branches change with the variation of the equivalence ratio, but the thermal mechanism always dominates in the diffusion flame branch. The interaction between flame branches is enhanced with the decrease of the distance between them. Both heat and radical exchange between flame branches contribute to the interaction. A new feature that does not exist in methane/air triple flame was observed in *n*-heptane/air triple flames, i.e. when the rich mixture equivalence ratio is higher, there are two peaks of CH concentration on the rich side of the diffusion flame branch, which leads to that some NO is formed beside the diffusion flame branch by the prompt route.

Keywords: Triple flame; NO_X; Laminar flame; Stratified combustion; Premixed flame

1. Introduction

Triple flames are of great importance for both industrial applications and fundamental combustion research. They play a significant role in flame attachment, lift-off, ignition and re-ignition processes of non-premixed systems. Many theoretical and experimental studies have been devoted to the structure and propagation of triple flames from various viewpoints [1–8]. However, fewer studies on NO_X formation in triple flames have been reported.

On the other hand, the formation of NO_X in combustion processes is of considerable practical interest because of the need to control pollutant formation. There have been many studies on the mechanism of NO_X formation. Miller and Bowman [9] presented an excellent review of NO_X formation mechanism. Based on the chemistry presented in this review paper, the formation of NO_X in methane/air double flames and two-dimensional laminar jet diffusion flames were respectively investigated by Nishioka et al. [10] and Ju and Niioka [11]. The effect of radiation heat loss on NO_X formation in counterflow flames was studied by several groups [12–16]. Atreya et al. [17] investigated the effect of change in flame structure on the formation of NO_X. An investigation on NO formation in an axisymmetric laminar diffusion flame was presented by Smooke et al. [18]. Naik and Laurendeau [19,20] studied NO formation in counterflow partially-premixed and non-premixed flames under sooting oxy-fuel and high pressure conditions. Sohn et al. [21] reported a study on the effects of pressure and air-dilution on NO formation in laminar counterflow diffusion flames of methane in high temperature air combustion. Xue and Aggarwal [22] and Bertra et al. [23] studied NO formation in *n*-heptane/air partially premixed flames. Naha and Aggarwal [24] investigated fuel effect on NO_X emissions in double flames. It has been quite clear from these studies that NO_X formation in a flame is closely related to the flame structure.

A triple flame consists of a diffusion flame embedded between a fuel lean and a fuel rich premixed flame. The structure of a triple flame is different from those of either the correspond-

* Corresponding author. Tel.: +1 (613) 991 0869; fax: +1 (613) 957 7869.
E-mail address: hongsheng.guo@nrc-cnrc.gc.ca (H. Guo).

1290-0729/$ – see front matter
doi:10.1016/j.ijthermalsci.2006.11.002

ing premixed flames, or traditional diffusion flames. Furthermore, because of the coexistence of the three flame branches, there are interactions among them that may affect the formation of NO_X in a triple flame. Our previous study [25] on NO_X formation in methane/air triple flames showed that NO_X formation in triple flames differs from in either premixed or diffusion flames.

n-heptane is a relatively heavy hydrocarbon fuel that is generally used to simulate diesel combustion. Study of NO_X formation in *n*-heptane triple flames is of help in understanding the mechanism of NO_X formation in diesel combustion. The purpose of the present paper is to numerically investigate NO_X formation in *n*-heptane/air triple flames. The discussion first focus on the results for two typical triple flames that exhibit the most significant features of triple flames. Then the effect of the variation in the equivalence ratio of the lean or rich mixture is examined. Finally the formation of NO_2 and N_2O is briefly discussed.

2. Numerical model

The flame configuration studied is an axisymmetric counterflow laminar flame. The governing equations can be found elsewhere [26]. The calculations were carried out with a code revised from that of Kee et al. [27]. Upwind and center difference schemes were used for the convective and diffusion terms, respectively, in all the governing equations. Adaptive refinement of meshes was done to obtain grid independent result. The pressure and the fresh mixture temperature were, respectively, 1 atm and 300 K. Radiation heat transfer was calculated by an optically thin method [28]. The distance between the two opposed jets was kept as 4.0 cm in all the simulations.

Potential and plug flow assumptions were alternately used in the literature for the free stream conditions in the simulation of counterflow flames. They usually generated similar qualitative results [29]. As a pure numerical study, the potential flow assumption was employed in this paper.

The reaction mechanism for the oxidation of *n*-heptane was one developed at the University of California, San Diego [30]. This mechanism has been validated by Li and Williams [31]. The nitrogen chemistry used was taken from GRI-Mech 3.0 [32], since it has been shown to offer reasonable prediction for NO formation at various flame conditions [20,33]. The combined mechanism consists of 303 elementary steps and 61 species. The thermal and transport properties were calculated by algorithms given in [34,35].

3. Results and discussion

The simulations were carried out for both triple and premixed flames for the sake of comparison. A counterflow triple flame (CFTF) was formed when a lean and a rich *n*-heptane/air mixture were respectively issued from the opposed nozzles, while a counterflow premixed flame (CFPF) was formed when the same mixtures were issued. A stretch rate of 60 s^{-1} was specified for all flames. This was an arbitrary choice. However, effect of the variation in stretch rate will be briefly discussed. In Figs. 1–9, the lean mixtures come from the left side, and the rich mixtures from the right side. The equivalence ratio is represented by ϕ.

3.1. Heat release rate distribution

To easily understand the characteristics of NO_X formation in triple flames, the heat release rate distribution of two typical counterflow *n*-heptane/air triple flames (Flames 1 and 2) is presented in Fig. 1. The equivalence ratios of the lean and rich *n*-heptane/air mixtures are 0.7 and 1.3 for Flame 1, and 0.7 and 2.0 for Flame 2. The reason to choose these two flames is that they both show typical triple flame structure, but the interaction among different flame branches varies for them.

The structure of triple flames is clearly illustrated. There are three heat release regions for each flame. The left one is due to the combustion of the lean mixture, while the right one is due to the rich mixture. These two heat release regions are named lean and rich premixed flame branches. Between these two flame branches, there is a relatively weak heat release region, named diffusion flame branch, which is because of the reaction of the excess oxygen from the lean mixture and the excess burning components from the rich mixture. Although not shown, the simulation indicated that similar to methane/air triple flames [25], all the fuel of the rich mixture is decomposed in the rich premixed flame, while the oxygen from the lean mixture can penetrate to the diffusion flame branch. The burning components transported from the rich premixed flame to the diffusion flame are some intermediate species, like CO and H_2. The diffusion branch of Flame 1 is located around the stagnation plane, while that of Flame 2 is located on the left side of the stagnation plane. The heat release rate in the diffusion flame branch of Flame 2 is higher than that of Flame 1, and the distance between the diffusion and rich premixed flame branches in Flame 2 is shorter than that in Flame 1. These are caused by the higher equivalence ratio of the rich mixture in Flame 2 than in Flame 1, leading to more burning components, such as H_2 and CO, are burnt in the diffusion flame branch of Flame 2.

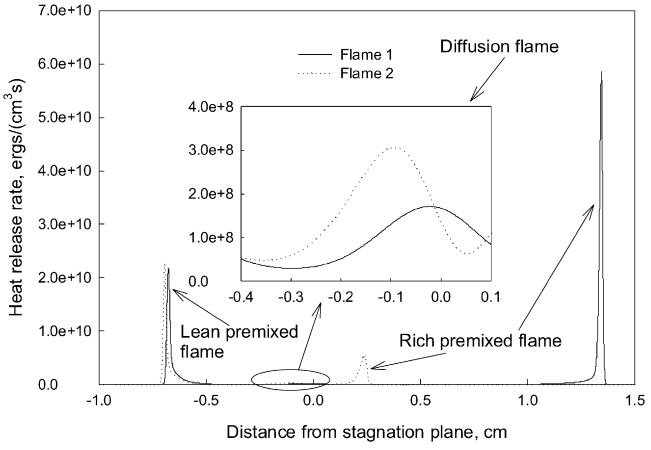

Fig. 1. Heat release rate distributions of two typical triple flames. Flame 1: $\phi_{lean} = 0.7$, $\phi_{rich} = 1.3$; Flame 2: $\phi_{lean} = 0.7$, $\phi_{rich} = 2.0$.

3.2. NO formation in two typical triple flames

It is well known that NO can be formed by the thermal, the N_2O intermediate, and the prompt routes [9–11], based on the initiation reactions by which molecular nitrogen is converted to atomic nitrogen or other intermediate species containing nitrogen element. The thermal NO formation is comprised of the three reactions: $N_2+O = N + NO$; $N + O_2 = NO + O$; and $N + OH = NO + H$; of which the first one is the initiation reaction. The N_2O intermediate route is initiated by the reactions: $N_2O\ (+M) = N_2 + O(+M)$; $N_2O + H = N_2 + OH$; $N_2O + O = N_2 + O_2$; and $N_2O + OH = N_2 + HO_2$; and then the formed N_2O is partially converted to NO. The prompt NO in hydrocarbon flames is initiated by the rapid reactions of hydrocarbon radicals with molecular nitrogen to form atomic nitrogen and species containing nitrogen element [9], and then the formed atomic nitrogen and other species containing nitrogen element are converted to NO by some reaction sequences. In addition, NO formation can also be initiated by the reactions of molecular nitrogen with some other hydrocarbon-free radicals, such as H, OH, H_2. These reactions include: $NH + N = N_2 + H$; $NH + NO = N_2 + OH$; $NNH = N_2 + H$; $NNH + M = N_2 + H + M$; $NNH + O_2 = HO_2 + N_2$; $NNH + O = OH + N_2$; $NNH + H = H_2 + N_2$; $NNH + OH = H_2O + N_2$; and $NNH + CH_3 = CH_4 + N_2$. Note that although the last reaction is initiated by CH_4, we also attribute it to this route due to NNH. This route to form NO is known as the NNH intermediate route [36]. To identify the relative importance of the four routes to NO formation, like in our previous studies [25, 37], four simulations were carried out for each flame. The first simulation (SIM1) was conducted by the full chemistry (GRI-Mech 3.0), while the second simulation (SIM2) was carried out by removing the initiation reactions of the prompt routes. In the third simulation (SIM3), the initiation reactions of both the prompt and the NNH intermediate routes were removed. All the initiation reactions of the prompt, the N_2O and the NNH intermediate routes were removed in the fourth simulation (SIM4). Consequently, NO obtained from SIM4 can be attributed to the thermal route. The difference in NO between SIM1 and SIM2 is attributed to the prompt route, and the difference between SIM2 and SIM3 is due to the NNH intermediate route. The NO contributed by the N_2O intermediate route is the difference between SIM3 and SIM4. It should be pointed out that this is an approximate method, since there may be interactions among different routes [20,25], as will be discussed later.

Fig. 2 illustrates the distribution of NO mole fraction in Flame 1 obtained by the four different simulations (SIM1–SIM4) and in the corresponding CFPFs obtained by the full NO chemistry. Because of the symmetry, only halves of the CFPFs are displayed. The summation of NO mole fractions obtained from the four separate simulations, in each of which the reaction scheme contains only the initial reactions of NO formation from one route, is also displayed to examine the independence of the four routes. It is observed that NO (full NO) in the CFTF starts to appear on both outer edges of the CFTF. At the positions corresponding to the two premixed flame branches (as shown in Fig. 1), the NO concentration rapidly increases. Then the concentration of NO gradually increases, and finally quickly rises again with the stagnation plane being approached. The maximum NO concentration is reached near the stagnation plane. In the regions corresponding to two premixed flame branches, the difference in the NO concentration between the CFTF and the CFPFs is negligible. However, the difference is increased in the region between the two premixed flame branches of the CFTF, with the maximum difference occurring near the stagnation plane.

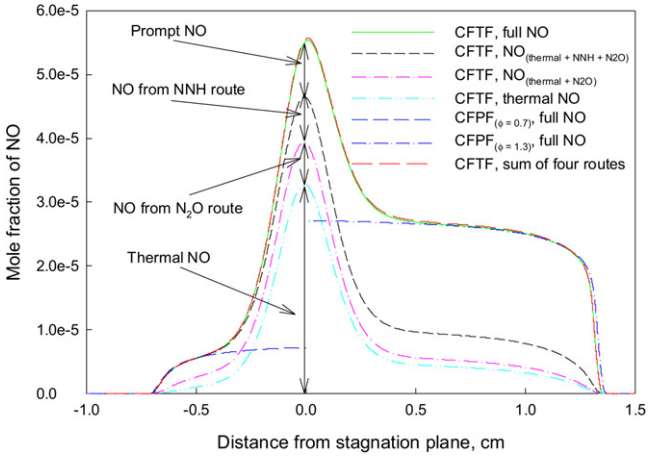

Fig. 2. NO concentration distributions in the triple flame with $\phi_{lean} = 0.7$ and $\phi_{rich} = 1.3$ and the corresponding CFPFs.

Fig. 2 also shows that most NO on the right side of the stagnation plane is produced by the prompt routes. In the lean premixed flame branch region, the NNH intermediate route contributes the most NO, followed by the N_2O intermediate route. However, approaching the stagnation plane from either right or left side, NO from the thermal route is gradually increased and finally exceeds those from other routes. Overall, the contributions from the N_2O and NNH intermediate routes are much smaller than from the thermal and the prompt routes in this flame.

There is a tiny difference between the NO mole fraction obtained from the full chemistry (green solid line) and the summation (red dashed line) of NO mole fraction obtained from the four separate simulations, in each of which the reaction scheme contains only the initial reactions of NO formation from one route. This implies that there is slight interaction between different NO formation routes. However, since the disparity is tiny and mainly happens on the right side where the contribution of the prompt route is much more significant than that of the thermal route, this interaction should not qualitatively affect the above conclusion, i.e. the prompt route dominates NO formation in the rich premixed flame branch. This will be further confirmed by the nitrogen consumption rate later. The interaction is negligible on the left side of the stagnation plane.

Fig. 3 shows the formation rate of NO in Flame 1. It is noted that there are three main NO formation regions, corresponding the three flame branches (Fig. 1). Similar to the NO mole fraction distribution, the difference in the formation rate between the CFTF and the corresponding CFPFs is negligible in the two

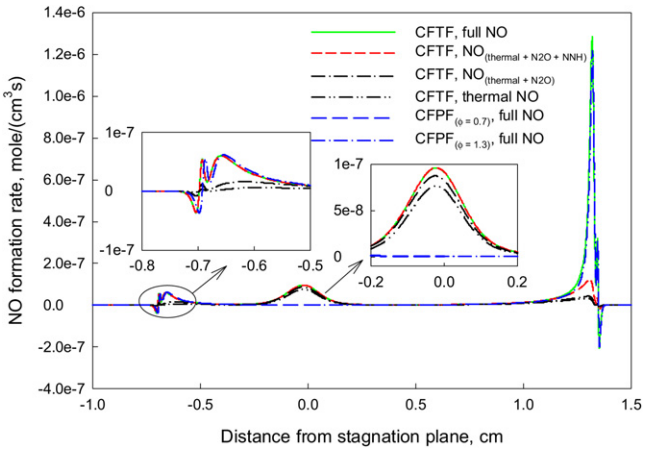

Fig. 3. NO formation rates in the flame with $\phi_{\text{lean}} = 0.7$ and $\phi_{\text{rich}} = 1.3$ and the corresponding CFPFs.

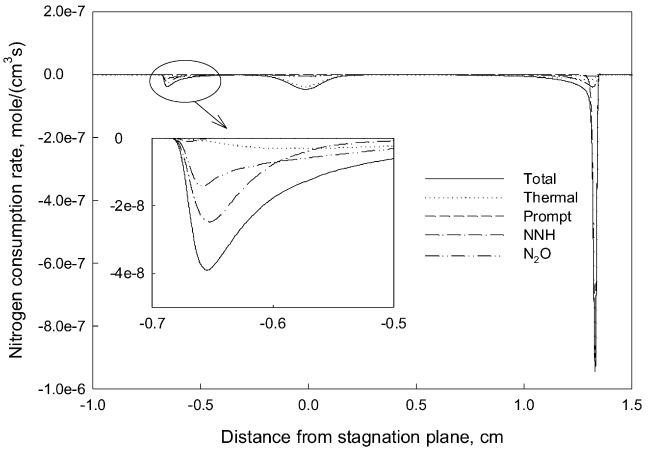

Fig. 4. Nitrogen consumption rates in the flame with $\phi_{\text{lean}} = 0.7$ and $\phi_{\text{rich}} = 1.3$.

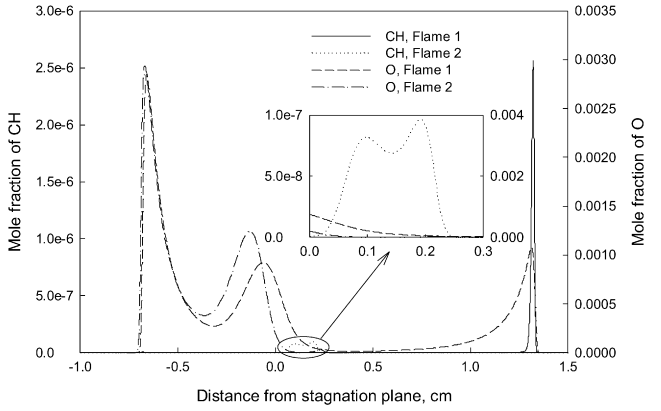

Fig. 5. Mole fractions of CH and O in two typical triple flames. Flame 1: $\phi_{\text{lean}} = 0.7$, $\phi_{\text{rich}} = 1.3$; Flame 2: $\phi_{\text{lean}} = 0.7$, $\phi_{\text{rich}} = 2.0$.

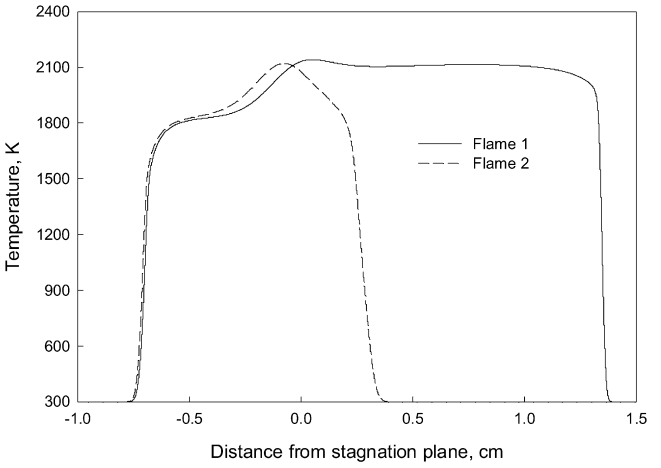

Fig. 6. Distribution of flame temperature in Flames 1 and 2. Flame 1: $\phi_{\text{lean}} = 0.7$, $\phi_{\text{rich}} = 1.3$; Flame 2: $\phi_{\text{lean}} = 0.7$, $\phi_{\text{rich}} = 2.0$.

premixed flame regions. However, the difference in the stagnation plane region becomes significant. In this region, the CFPFs almost do not produce NO, while the CFTF does significantly. This indicates that a triple flame produces more NO than the corresponding premixed flames due to the appearance of the diffusion flame branch. Similarly, it is further shown that the prompt route contributes most NO in the rich premixed flame branch of the CFTF. However, in the diffusion flame branch, the thermal route dominates. In the reaction zone of the lean premixed flame branch, the NNH intermediate route is the most significant one.

The above discussion on the relative contribution is based on the technique that gradually switches off the initiation molecular nitrogen conversion reactions of different routes. Since there is tiny interaction among different routes, the above conclusion needs to be further examined. Fig. 4 displays the molecular nitrogen consumption rates by the thermal, prompt, N_2O and NNH intermediate routes, obtained from the simulation using the full chemistry (SIM1). It shows that molecular nitrogen is mainly consumed by the prompt route in the rich premixed flame, and by the NNH intermediate route in the lean premixed flame. In the diffusion flame branch, the thermal route dominates the conversion of nitrogen. This confirms the previous conclusion on the relative contributions of different routes to NO formation in Flame 1, i.e. the prompt, the thermal and the NNH intermediate route contribute most NO formation, respectively, in the rich premixed, the diffusion and the lean premixed flame branches. Therefore, the method we used captured the qualitative feature of NO formation in a triple flame.

The variation of the relative contributions of different routes in the three flame branches is caused by the specific structure of Flame 1. The most significant initiation reactions of NO formation by the thermal and prompt routes are, respectively, $N + NO = N_2 + O$ and $CH + N_2 = HCN + N$ [9,10,20,25]. Therefore, the existence of radicals O and CH is crucial for the formation of NO through the thermal and prompt routes. Fig. 5 gives the distributions of radicals O and CH in Flames 1 and 2. The prompt route contributes most NO in the rich premixed branch of Flame 1, because of the significant amount of CH there. In the diffusion flame branch, there is no radical CH, leading to the negligible contribution of the prompt route. Temperature reaches its maximum value, as shown in Fig. 6, and there is certain amount of radical O in the diffusion flame branch (located near the stagnation plane). Consequently, the thermal route dominates the formation of NO in the diffusion

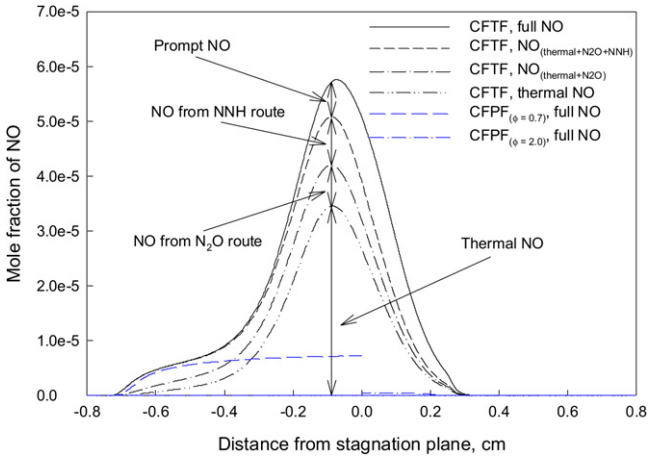

Fig. 7. NO mole fractions in the flame with $\phi_{\text{lean}} = 0.7$ and $\phi_{\text{rich}} = 2.0$ and the corresponding CFPFs.

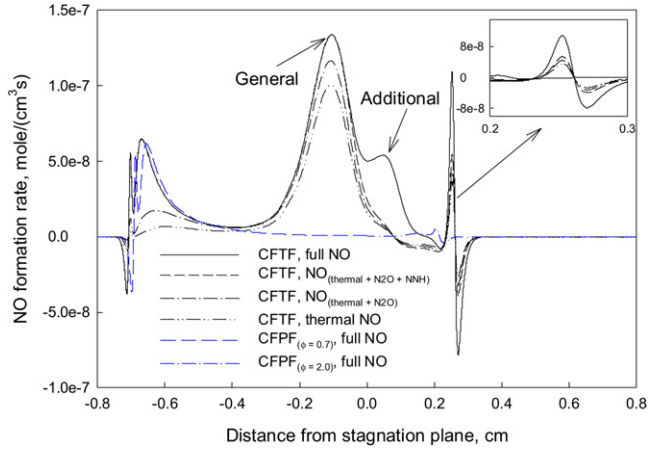

Fig. 8. NO formation rates in the flame with $\phi_{\text{lean}} = 0.7$ and $\phi_{\text{rich}} = 2.0$ and the corresponding CFPFs.

flame branch. In the reaction zone of the lean flame branch, due to the low temperature and the low concentration of radical CH, the thermal and prompt routes contribute little to NO formation. On the other hand, relatively the NNH intermediate route contributes more NO in the lean premixed flame branch, since the most significant initiation reactions of this route are $\text{NNH} \Leftarrow \text{N}_2 + \text{H}$ and $\text{NNH} + \text{M} \Leftarrow \text{N}_2 + \text{H} + \text{M}$ and radical H appears in all three flame branches. These NO formation characteristics in Flame 1 are qualitatively consistent with those in a methane/air triple flame [25], in which the interaction among different flame branches is negligible.

Figs. 7 and 8 display the distributions of NO mole fraction and formation rate in Flame 2 (note that the scale of the horizontal axis in Figs. 7–9 is different from in Figs. 1–6, so that the figures are not crowded). They are qualitatively similar to those of Flame 1. However, some important new features are observed. The first new feature is that the NO concentration and production rate are significantly higher than those of the corresponding CFPFs not only in the stagnation plane region, but also in the rich premixed flame branch region. The NO formation region in the rich premixed flame branch is further away from the stagnation plane than that in the corresponding rich

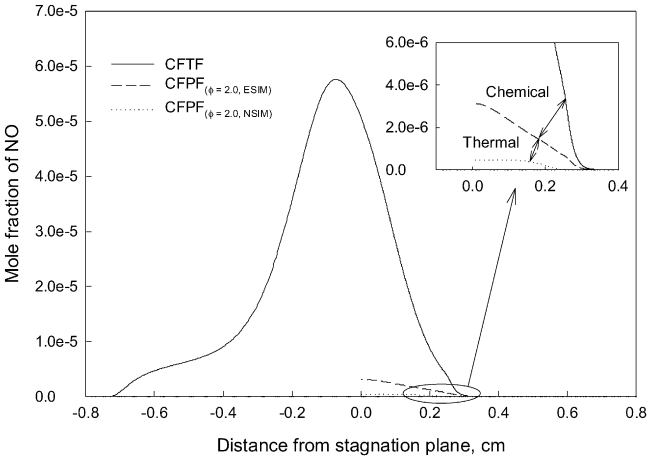

Fig. 9. NO mole fractions of Flame 2 ($\phi_{\text{lean}} = 0.7$ and $\phi_{\text{rich}} = 2.0$) and the corresponding rich CFPF obtained from NSIM and ESIM.

CFPF. These differences are caused by the fact that the rich mixture of this CFTF is richer than that of Flame 1. Therefore, the rich premixed flame branch in Flame 2 is closer to the diffusion flame branch than in Flame 1. The shorter distance enhances the interaction between the diffusion and rich premixed flame branches. This interaction leads to that the combustion intensity and NO formation rate in the rich branch of this CFTF are higher than those in the corresponding rich CFPF.

The interaction between the diffusion and rich premixed flame branches in a triple flame can be caused by the heat transfer, named thermal interaction, and radical exchange, named chemical interaction. To identify the relative contributions of these two interactions, as in our previous studies [25,38] for triple flames, we did an extra simulation (ESIM) for the corresponding rich CFPF of Flame 2. In this extra simulation, the symmetrical boundary condition for the energy conservation equation on the stagnation plane was replaced by a fixed value that is the maximum temperature of Flame 2. All other conditions are the same as those in the normal simulation (NSIM). Therefore, the heat transfer from the stagnation plane to the primary reaction zone in this extra simulation is similar to that from the diffusion flame branch to the rich premixed flame branch in Flame 2. However, there is no significant radical exchange between the stagnation plane and the primary reaction zone in the rich CFPF of the extra simulation. Accordingly, the difference between Flame 2 and the rich CFPF of ESIM is caused by the chemical interaction in the triple flame, and that between the rich CFPF of ESIM and the rich CFPF of NSIM is because of the thermal interaction. Fig. 9 shows the NO mole fraction of Flame 2 and the corresponding rich CFPF obtained by NSIM and ESIM. It is demonstrated that the thermal and chemical interaction play similar roles in enhancing the combustion and NO formation in the rich premixed flame branch of Flame 2. This conclusion is also consistent with what we obtained for the methane/air triple flames with stronger interaction between different branches [25].

The second new feature noted in Flame 2 is that there is an additional NO formation region, indicated by “Additional”

in Fig. 8, in addition to the three corresponding flame regions observed in Flame 1. This additional NO formation region is just beside (right-hand side) the diffusion flame branch (indicated by "General"). The prompt route (the difference between the black solid and dashed lines) dominates the formation of NO in this region. This is caused by the specific distribution of radical CH in Flame 2. As shown in Fig. 5, there are two peaks for CH concentration on the right-hand side of stagnation plane in Flame 2. The first corresponds to the rich premixed flame branch, and the second one is located beside stagnation plane. Since the fresh mixture from the right-hand side is very rich, there is not enough oxygen to convert all the acetylene (C_2H_2) in the rich premixed flame branch. As a result, acetylene can be transported to the region beside the diffusion flame branch where radical O is met. Then acetylene is quickly converted to CH by the reactions $O + C_2H_2 \Rightarrow CO + CH_2$ and $CH + H_2 \Leftarrow H + CH_2$, forming the second peak of CH concentration beside the diffusion flame branch. This second peak of CH concentration leads to the additional NO formation region beside the diffusion flame branch mainly by the prompt route. This phenomenon of double CH concentration peaks on the right side of stagnation plane in Flame 2 is similar to that numerically observed by Xue and Aggarwal [22] for *n*-heptane/air double flames and experimentally by Naik and Laurendeau [39] for methane/air partially premixed flames at pressures above 3 atm. However, it does not happen in Flame 1 and in methane/air triple flames [25]. We attribute this NO formation region to the diffusion flame branch, since it is due to the transportation of hydrocarbon radicals to the diffusion flame region. It is noted that the overall contribution of the thermal route is still dominant in the diffusion branch of this triple flame.

NO formation for Flame 1 at other stretch rates was also calculated. It was found that similar to methane/air triple flames [25], the variation of stretch rate does not affect the qualitative feature of NO formation in a triple flame, although the absolute amount of NO formed changes when stretch rate varies. Therefore, details of the effect of stretch rate on NO formation will not be discussed in this paper.

3.3. NO formation in other triple flames

Fig. 10 shows NO emission index, defined as the ratio of the NO formed to the fuel consumed, in some other triple flames. The equivalence ratio of the lean mixture in Fig. 10(a) is 0.7, while that of the rich mixture in Fig. 10(b) is 1.3. It is demonstrated that the variation of either the lean or the rich mixture equivalence ratio affects the formation of NO.

When the equivalence ratio of the lean mixture is fixed as 0.7 (Fig. 10(a)), with the increase of the rich mixture equivalence ratio, the NO emission index first decreases, then slightly increases, and finally reduces to an almost constant value. As the equivalence ratio of the rich mixture is 1.1, the thermal route contributes most NO. This is because the temperature in the rich flame branch is higher and the thermal route dominates the formation of NO in the rich premixed flame branch of this triple flame. With the increase of the rich mixture equivalence ratio from 1.1 to 1.3, the drop of NO emission index is because the combustion intensity and temperature of the rich premixed flame reduce. This can be shown by the sharp decrease of the contribution of the thermal route when the rich mixture equivalence ratio rises from 1.1 to 1.3. Our simulation indicates that the thermal route dominates the NO formation in the rich premixed flame branch only when the equivalence ratio of the rich mixture is smaller than 1.2. This is different from the conclusion for *n*-heptane/air double flames obtained by Xue and Aggarwal [22], who suggested that the thermal route generally contributes more NO than the prompt route in the rich premixed zone of a double flame. This difference may be caused by the method to evaluate the relative contributions of different routes. Xue and Aggarwal [22] attributed all NO from the reactions: $N_2 + O = N + NO$; $N + O_2 = NO + O$; and $N + OH = NO + H$ to the thermal route. This method overestimates the contribution of the thermal NO, since part of the atomic nitrogen participating in the last two reactions is from the reaction $CH + N_2 = HCN + N$ (the most significant initiation reaction of the prompt NO formation) and the later conversion of HCN. Like [20,25,37], the present paper determines the relative contributions of different routes based on how molecular nitrogen is converted to atomic nitrogen or species containing element nitrogen. Therefore, the element nitrogen from

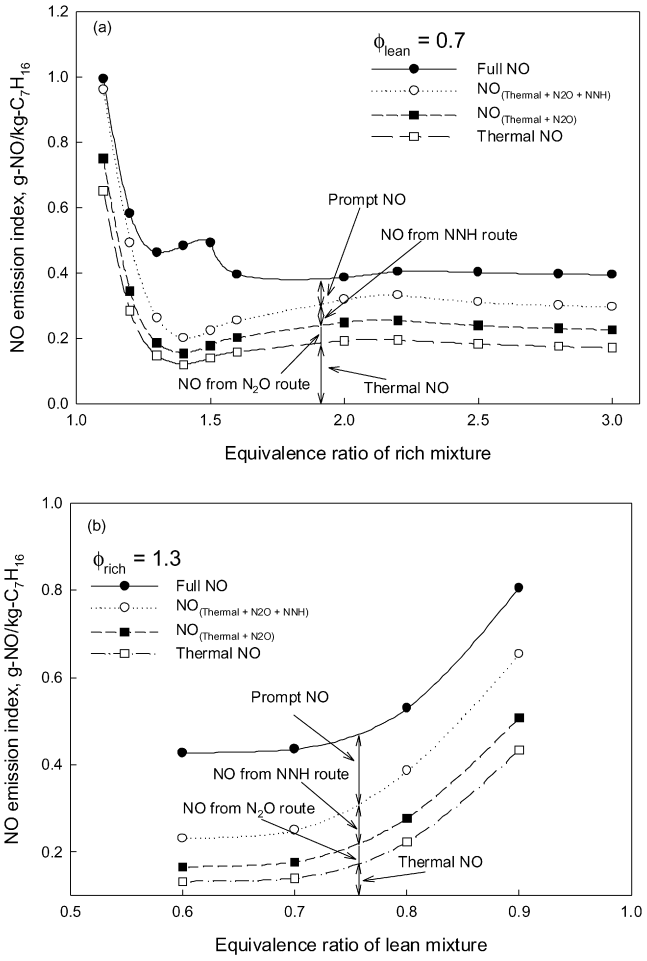

Fig. 10. Effect of lean or rich mixture equivalence ratio on NO formation.

different routes participating in the reactions $N + O_2 = NO + O$ and $N + OH = NO + H$ is successfully separated.

When the rich mixture equivalence ratio rises from 1.3 to 1.5, the contribution of the prompt route in the rich premixed flame branch increases, leading to the rise of total NO formation. With the increase of the rich mixture equivalence ratio from 1.5 to 1.6, the decrease of NO formation is caused by the significantly reduced combustion intensity in the rich premixed flame branch. As the rich mixture equivalence ratio is further increased, the contribution of the rich premixed branch to the NO formation of a triple flame becomes very small, and the formation of NO in a triple flame is dominated by that in its lean and diffusion flame branches. Accordingly, the NO emission index becomes almost constant when the equivalence ratio is greater than 1.6. The slight increases of the thermal NO formation is because more fuel components are burnt in the diffusion flame branch, when the rich mixture equivalence ratio rises from 1.4 to 2.2.

The variation of the rich mixture equivalence ratio also affects the NO formation mechanism in the diffusion flame branch. When the equivalence ratio of the rich mixture is low, little hydrocarbon radical can be transported to the diffusion flame branch. Therefore, the prompt route contributes negligible to NO formation in the diffusion flame branch, like in Flame 1. This is similar to that for methane/air triple flames [25]. As the rich mixture equivalence ratio is increased, the phenomenon of double peaks of CH concentration appears, leading to that some NO is formed by the prompt route beside the diffusion flame branch, such as in Flame 2. This phenomenon does not happen in methane/air triple flames. The contribution of the prompt route does not exceed that of the thermal route in the diffusion flame branch until the rich mixture equivalence ratio reaches 3.0, at which the rich premixed flame branch and the diffusion flame branch almost merge. The thermal route always contributes most of NO in the diffusion flame branch. This differs from the conclusion for *n*-heptane/air double flames obtained by Xue and Aggarwal [22], who indicated that the prompt route is the primary contributor for NO formation in the diffusion flame region of a *n*-heptane/air double flame.

When the equivalence ratio of the rich mixture is fixed as 1.3 (Fig. 10(b)), with the decrease of the lean mixture equivalence ratio, the NO emission index monotonically reduces. It is due to the reduction in the combustion intensity in the lean premixed flame branch. The contribution of the thermal route also reduces with the decrease of the lean mixture equivalence ratio, since the temperature is higher and the thermal route dominates the NO formation when the equivalence ratio of the lean mixture is close to 1.0. This is similar to that observed for methane/air triple flame [25].

The formation of NO_2 and N_2O in the two typical triple flames was also examined. It was found that the characteristics of NO_2 and N_2O formation in *n*-heptane/air triple flames are qualitatively similar to those in methane/air triple flames [25]. Therefore, the results and detailed discussion will not be given in this paper.

4. Conclusions

We have investigated NO_X formation in counterflow *n*-heptane/air triple flames by numerical simulation. The characteristics of NO_X formation in triple flames were compared to those in corresponding counterflow premixed flames. The mechanism of NO formation in triple flames was analyzed by a method of strategically turning-off initial molecular nitrogen conversion reactions of different routes. The results suggest that a triple flame produces more NO and NO_2 than the corresponding premixed flames due to the appearance of the diffusion flame branch and the interaction between flame branches. The interaction between flame branches is enhanced with the decrease of the distance between them. Calculations that separated the thermal and chemical effects show that both heat and radical exchange between flame branches contribute to the interaction. The variation of the equivalence ratio affects the relative contributions of different routes to NO formation in the premixed flame branches, but the thermal route always dominates in the diffusion flame branch. When the rich mixture equivalence ratio is not high enough, there is only one CH peak appearing on the rich side of the diffusion flame branch, and prompt route contributes little to NO formation in the diffusion flame branch. However, when the rich mixture equivalence ratio is higher, there are two peaks of CH concentration on the rich side of the diffusion flame branch, which leads to that some NO is formed beside the diffusion flame branch by the prompt route. The characteristics of NO_2 and N_2O formation in *n*-heptane/air triple flames are qualitatively similar to those in methane/air triple flames.

Acknowledgement

We thank Mr. M. Moore and Mr. J. Daniels for conducting some of the simulations.

References

[1] H. Phillips, Flame in a buoyant methane layer, Proc. Combust. Inst. 10 (1965) 1277–1283.
[2] A. Liñán, A. Crespo, An asymptotic analysis of unsteady diffusion flames for large activation energies, Combust. Sci. Technol. 14 (1976) 95–117.
[3] J.W. Dold, Flame propagation in a nonuniform mixture: analysis of a slowly varying triple flame, Combust. Flame 76 (1989) 71–88.
[4] T. Echekki, J.H. Chen, Structure and propagation of methanol–air flames, Combust. Flame 114 (1998) 231–245.
[5] T. Plessing, P. Terhoeven, N. Peters, M.S. Mansour, An experimental and numerical study of a laminar triple flame, Combust. Flame 115 (1998) 335–353.
[6] P.N. Kīoni, K.N.C. Bray, D.A. Greenhalgh, B. Rogg, Experimental and numerical studies of a triple flame, Combust. Flame 116 (1999) 192–206.
[7] H.G. Im, J.H. Chen, Structure and propagation of triple flames in partially premixed hydrogen–air mixtures, Combust. Flame 119 (1999) 436–454.
[8] R.D. Lockett, B. Boulanger, S.C. Harding, D.A. Greenhalgh, The structure and stability of the laminar counter-flow partially premixed methane/air triple flame, Combust. Flame 119 (1999) 109–120.
[9] J.A. Miller, C.T. Bowman, Mechanism and modeling of nitrogen chemistry in combustion, Prog. Energy Combust. Sci. 15 (1989) 287–338.
[10] M. Nishioka, S. Nakagawa, Y. Ishikawa, T. Takeno, NO emission characteristics of methane–air double flame, Combust. Flame 98 (1994) 127–138.

[11] Y. Ju, T. Niioka, Computation of NO_X emission of a methane–air diffusion flame in a two-dimensional laminar jet with detailed chemistry, Combust. Theory Modelling 1 (1997) 243–258.
[12] A. Varnos, B.J. Hall, Influence of radiative loss on nitric oxide formation in counterflow diffusion flames at high pressure, Combust. Flame 93 (1993) 230–238.
[13] J. Wang, T. Niioka, The effect of radiation reabsorption on NO formation in CH_4/air counterflow diffusion flames, Combust. Theory Modelling 5 (2001) 385–398.
[14] J. Wang, T. Niioka, Numerical study of radiation reabsorption effect on NO_X formation in CH_4/air counterflow premixed flames, Proc. Combust. Inst. 29 (2002) 2211–2218.
[15] X.L. Zhu, J.P. Gore, Radiation effects on combustion and pollutant emissions of high-pressure opposed flow methane/air diffusion flames, Combust. Flame 161 (2005) 118–130.
[16] S.V. Naik, N.M. Laurendeau, J.A. Cooke, M.D. Smooke, Effect of radiation on nitric oxide concentration under sooting oxy-fuel conditions, Combust. Flame 134 (2003) 425–431.
[17] A. Atreya, H.K. Kim, T. Shamim, J. Suh, The effect of changes in the flame structure on the formation and destruction of soot and NO_X in radiating diffusion flames, Proc. Combust. Inst. 26 (1996) 2181–2189.
[18] M.D. Smooke, A. Ern, M.A. Tanoff, B.A. Valdati, R.K. Mohammed, D.F. Marran, M.B. Long, Computational and experimental study of NO in an axisymmetric laminar diffusion flame, Proc. Combust. Inst. 26 (1996) 2161–2170.
[19] S.V. Naik, N.M. Laurendeau, Quantitative laser-saturated fluorescence measurements of nitric oxide in counter-flow diffusion flames under sooting oxy-fuel conditions, Combust. Flame 129 (2002) 112–119.
[20] S.V. Naik, N.M. Laurendeau, LIF measurements and chemical kinetic analysis of nitric oxide formation in high-pressure counterflow partially premixed and non-premixed flames, Combust. Sci. Technol. 176 (2004) 1809–1853.
[21] C.H. Sohn, I.M. Jeong, S.H. Chung, Numerical study of the effects of pressure and air-dilution on no formation in laminar counterflow diffusion flames of methane in high temperature air, Combust. Flame 130 (2002) 83–93.
[22] H. Xue, S.K. Aggarwal, NO_X emissions in n-heptane/air partially premixed flames, Combust. Flame 132 (2003) 723–741.
[23] P. Berta, S.K. Aggarwal, I.K. Puri, An experimental and numerical investigation of n-heptane/air counterflow partially premixed flames and emission of NO_X and PAH species, Combust. Flame 145 (2006) 740–764.
[24] S. Naha, S.K. Aggarwal, Fuel effects on NO_X emissions in partially premixed flames, Combust. Flame 139 (2004) 90–105.
[25] H. Guo, F. Liu, G.J. Smallwood, A numerical study on NO_X formation in laminar counterflow CH_4/air triple flames, Combust. Flame 143 (2005) 303–311.
[26] V. Giovangigli, M.D. Smooke, Extinction of strained laminar flames with complex chemistry, Combust. Sci. Tech. 53 (1987) 23–49.
[27] R.J. Kee, J.F. Grcar, M.D. Smooke, J.A. Miller, A Fortran program for modelling steady laminar one-dimensional premixed flames, Report No. SAND85-8240, Sandia National Laboratories, 1985.
[28] H. Guo, Y. Ju, K. Maruta, K. Niioka, F. Liu, Radiation extinction limit of counterflow premixed lean methane–air flames, Combust. Flame 109 (1997) 639–646.
[29] R. Chen, R.L. Axelbaum, Scalar dissipation rate at extinction and the effects of oxygen-enriched combustion, Combust. Flame 142 (2005) 62–71.
[30] UCSD, http://maeweb.ucsd.edu/~combustion/cermech/.
[31] S.C. Li, F.A. Williams, Counterflow heptane flame structure, Proc. Comb. Inst. 28 (2000) 1031–1038.
[32] G.P. Smith, D.M. Golden, M. Frenklach, N.W. Moriarty, B. Eiteneer, M. Goldenberg, C.T. Bowman, R.K. Hanson, S. Song, W.C. Gardiner Jr, V.V. Lissianski, Z. Qin, http://www.me.berkeley.edu/gri_mech/.
[33] A.V. Menon, S.-Y. Lee, M.J. Linevsky, T.A. Litzinger, R.J. Santoro, Addition of NO_2 to a laminar premixed ethylene–air flame: effect on soot formation, Proc. Comb. Inst. 31 (2006), in press.
[34] R.J. Kee, J. Warnatz, J.A. Miller, A Fortran computer code package for the evaluation of gas-phase viscosities, conductivities, and diffusion coefficients, Report No. SAND 83-8209, Sandia National Laboratories, 1983.
[35] R.J. Kee, J.A. Miller, T.H. Jefferson, A general-purpose, problem-independent, transportable, Fortran chemical kinetics code package, Report No. SAND 80-8003, Sandia National Laboratories, 1980.
[36] G.J. Rørtveit, J.E. Hustad, S. Li, F.A. Williams, Effects of diluents on NO_X formation in hydrogen counterflow flames, Combust. Flame 130 (2002) 48–61.
[37] H. Guo, G.J. Smallwood, F. Liu, Y. Ju, Ö.L. Gülder, The effect of hydrogen addition on flammability limit and NO_X emission in ultra-lean counterflow CH_4/air premixed flames, Proc. Comb. Inst. 30 (2005) 303–311.
[38] H. Guo, F. Liu, G.J. Smallwood, A numerical study of laminar methane/air triple flame in two-dimensional mixing layers, Int. J. Thermal Sci. 45 (2006) 586–594.
[39] S.V. Naik, N.M. Laurendeau, LIF measurements and chemical kinetic analysis of methylidyne formation in high-pressure counter-flow partially premixed and non-premixed flames, Appl. Phys. B 79 (2004) 891–905.